Bone 124 (2019) 14–21

Contents lists available at ScienceDirect

Bone

journal homepage: www.elsevier.com/locate/bone

Case Report

Phenotype and response to growth hormone therapy in siblings with *B4GALT7* deficiency

Carla Sandler-Wilson[a], Jennifer A. Wambach[a,*], Bess A. Marshall[a,b], Daniel J. Wegner[a], William McAlister[c], F. Sessions Cole[a,b], Marwan Shinawi[a]

[a] Edward Mallinckrodt Department of Pediatrics, Washington University School of Medicine, St. Louis Children's Hospital, St. Louis, MO 63110, USA
[b] Department of Cell Biology and Physiology, Washington University School of Medicine, St. Louis Children's Hospital, St. Louis, MO 63110, USA
[c] Mallinckrodt Institute of Radiology, Washington University School of Medicine, St. Louis Children's Hospital, St. Louis, MO 63110, USA

ARTICLE INFO

Keywords:
B4GALT7
Spondylodysplastic Ehlers-Danlos syndrome
Larsen of Reunion Island syndrome
Growth hormone
Proteoglycan

ABSTRACT

B4GALT7 encodes beta-1,4-galactosyltransferase which links glycosaminoglycans to proteoglycans in connective tissues. Rare, biallelic variants in *B4GALT7* have been associated with spondylodysplastic Ehlers-Danlos and Larsen of Reunion Island syndromes. Thirty patients with *B4GALT7*-related disorders have been reported to date with phenotypic variability. Using whole exome sequencing, we identified male and female siblings with biallelic, pathogenic *B4GALT7* variants and phenotypic features of spondylodysplastic Ehlers-Danlos syndrome as well as previously unreported skeletal characteristics. We also provide detailed radiological characterization and describe the siblings' responses to growth hormone treatment. Our report extends the phenotypic spectrum of *B4GALT7*-associated spondylodysplastic Ehlers-Danlos syndrome and reports results of growth hormone treatment for patients with this rare disorder.

1. Introduction

B4GALT7 (MIM# 604327) encodes beta-1,4-galactosyltransferase, a 327-amino acid transmembrane enzyme that catalyzes the addition of galactose to xylose in the tetrasaccharide linkage region of proteoglycans [1]. This enzyme is critical for the O-linked glycosylation-mediated functions of proteoglycans, a major component of the extracellular matrix. Pathogenic variants in *B4GALT7* reduce expression or disrupt catalytic activity of beta-1,4-galactosyltransferase and result in defective extracellular matrix [1,2]. Beta-1,4-galactosyltransferase deficiency has been associated in humans with the spondylodysplastic type of Ehlers-Danlos syndrome (spEDS) (MIM# 130070), a connective tissue disorder characterized by skeletal abnormalities, most notably radioulnar synostosis, short stature, joint hypermobility, and dysmorphic facial features as well as developmental delays [1]. Targeted genetic disruption of *B4GALT7* in mice results in sparse hair and severe skin lesions consistent with the human phenotypic characteristics of hyperkeratosis and acanthosis as well as post-natal growth restriction, enlarged intestinal crypts, smaller litter sizes, abnormal anterior pituitary function, and shortened lifespan [3–5].

Thirty individuals with biallelic, pathogenic variants in *B4GALT7* have been reported, 22 of whom reside on Reunion Island in the southern Indian Ocean. Despite phenotypic variability among these individuals, common features include radioulnar synostosis, short stature, joint hypermobility, hyperelastic skin, and hypotonia (Table 1) [1,6–12].

We describe male and female siblings with rare, biallelic, pathogenic variants in *B4GALT7* and their responses to growth hormone treatment for short stature, summarize the phenotypes associated with biallelic, pathogenic *B4GALT7* variants, and highlight the unique phenotypic characteristics of these 2 siblings.

2. Materials and methods

After approval by the Human Research Protection Office at Washington University School of Medicine, we obtained informed written consent for publication including photographs from the siblings' parents.

Clinical exome sequencing was performed by GeneDx (Gaithersburg, MD) using Agilent SureSelect XT2 All Exon V4 Kit, an Illumina HiSeq 2000 device, and 100 bp paired-end reads. Sequence reads were aligned to the UCSC build hg19 reference sequence (genome.ucsc.edu). The mean depth of coverage of known protein-coding RefSeq genes was 205X with quality threshold of 98.3%.

* Corresponding author at: Division of Newborn Medicine, Box 8116, Washington University School of Medicine, 660 S. Euclid Avenue, St. Louis, MO 63110, USA.
E-mail address: wambachj@wustl.edu (J.A. Wambach).

https://doi.org/10.1016/j.bone.2019.03.029
Received 26 December 2018; Received in revised form 13 March 2019; Accepted 22 March 2019
Available online 23 March 2019
8756-3282/

Table 1
Clinical characteristics for patients with B4GALT7 deficiency.

Publication year	2019	2019	2017 [6]	2016 [7]	2016 [1]	2016 [1]	2013 [8]	2004 [9]	2004 [9]	1987 [10]	2015 [11]	Total	%
Genotype	p.Arg270Cys p.Arg141Trp	p.Arg270Cys p.Arg141Trp	Homozygous p.Glu277[a]	Homozygous p.Cys324Ser	p.Arg270Cys p.Arg141Trp	p.His93Profs[a]73 p.Cys214Tyr	p.Arg270Cys p.Leu41Pro	Homozygous p.Arg270Cys	Homozygous p.Arg270Cys	p.Leu205Pro p.Ala186Asp	Homozygous p.Arg270Cys		
Country of origin	USA	USA	Morocco	Mexico	Not reported	NR	NR	Qatar	Qatar	Denmark	Reunion Island		
Gender (M/F)	M	F	F	F	F	M	M	F	M	M	11 M/11 F		
Birth weight (grams)	2780	2334	Normal	1665[a]	2580	2795	2970	2300	2500	3030	NR		
Age at diagnosis (years)	10	4	30	5	13	3.5	10	2	33	4.75	4–46		
Short stature	+	+	+	+	+	+	+	+	+	+	19/19	29/29	100
Hypermobility/frequent joint dislocations	+	+	+	+	+	+	+	+	+	+	NR	10/10	100
Hypotonia	+	+	+	+	+	+	+	+	+	+	NR	10/10	100
Hyperelastic skin	+	+	+	+	+	+	+	+	+	+	21/22	31/32	97
Motor delay	+	+	+	+	+	+	−	+	+	+	NR	9/10	90
Pes planus/equinovarus/valgus	+	+	+	+	+	+	+	−	+	+	NR	9/10	90
Abnormal/delayed healing	+	−	+	+	+	+	+	−	+	+	NR	8/10	80
Bowing of limbs	+	+	−	−	+	+	+	+	+	−	NR	7/10	70
Cognitive delay/learning disabilities	+	+	−	+	−	+	+	+	+	+	12/22	20/32	63
Growth hormone deficiency	+	+	−	NR	NR	NR	+	NR	NR	−	NR	3/5	60
Osteopenia	+	−	+	NR	−	+	−	+	−	+	NR	5/9	56
Radio-ulnar synostosis	+	+	−	−	+	+	+	+	+	+	10/22	18/32	56
Blue sclerae	+	+	+	−	+	+	−	−	−	−	NR	5/10	50
Chest wall deformity	+	−	−	+	−	−	+	−	−	−	5/22	8/32	25
Coronal clefts (vertebrae)	+	+	−	−	−	−	−	−	−	−	NR	2/10	20
Fused sagittal sutures (skull)	+	+	−	−	−	−	−	−	−	−	NR	2/10	20
Cleft palate	+	−	−	−	−	+	−	−	−	−	1/22 (female)	3/32	9

NR: not reported.
[a] Induced at 34 weeks' for IUGR.

XomeAnalyzer was used to evaluate sequence differences between the siblings, parental samples, and reference sequence error. Variants were confirmed with Sanger sequencing, and pathogenicity was predicted with combined annotation dependent depletion scores (CADD) [13].

Growth hormone was assayed using an Electrochemiluminescence Immunoassay (ECLIA) sandwich principle calibrated to the World Health Organization National Institute for Biological Standards and Control, 2nd International Standard, 98/574 (Potters Bar, Hertfordshire, EN6 3QG).

2.1. Clinical report

2.1.1. Family history

The father is of French descent, and the mother's ancestry is not known as the maternal grandmother was adopted. The mother's adult height is 162 cm (25–50th percentile) [14], and the father's adult height is 188 cm (90–95th percentile) [14]. Family history is negative for skeletal dysplasia. Father has neither musculoskeletal complaints nor chronic medical conditions. Mother has suffered from frequent knee dislocations, and maternal grandmother has spinal stenosis which required multiple operations including rod placement for spinal support and age-related osteopenia treated with oral bisphosphonate therapy.

2.1.2. Male sibling

The male sibling was born at term: birth weight 2780 g (9th percentile) and length 44 cm (< 1st percentile, −2.7 S.D.) [14]. At birth, he was noted to have cleft palate, brachycephaly, broadened and flat nasal bridge, retrognathia, overlapping superior helices, axial hypotonia, and spasticity of all four extremities with brisk reflexes, more pronounced in the upper extremities than the lower extremities. Contractures were present at the elbows and ankles. Skeletal survey performed at 3 weeks of age demonstrated butterfly vertebrae at T7 and T8, coronal cleft deformities of the thoracic and lumbar spine, bilateral dislocation of the radial heads with hypoplasia of the distal radii, bowing of the proximal ulnae, elongated distal phalanges of all fingers, and elongated fibulae compared to tibiae (Fig. 1, Fig. S1). Subsequent bone surveys continued to show minimal metacarpal shortening relative to phalanges in addition to deformities of the proximal carpal row and positive ulnar variance; radiograph of his right foot demonstrated shortened fourth metatarsal and minimal deformity of the distal phalanx of the great toe (Fig. S2). Subsequent bone surveys also noted multiple areas of abnormal bone fusion including partial fusion of C2–3 and C4–5 neural arches (Fig. S3) and closure of the sagittal suture with an asymmetric skull (Fig. S4). Voiding cystourethrography performed due to renal ultrasound findings of hydronephrosis demonstrated grade IV vesicoureteral reflux. Chest computed axial tomography scan at age 5 years was notable for anterior left chest deformity (Fig. S5). Brain magnetic resonance imaging (MRI) at age 6 weeks was unremarkable. Chromosomal microarray (CMA) revealed a ~719 kb duplication on 9p24.3 (46,587 to 765,259 (hg19)) inherited from his asymptomatic father that contains the following genes: *FOXD4*, *C9orf66*, *DOCK8*, *KANK1*, and *CBWD1* [12]. None of these genes has been associated with skeletal abnormalities or with features of *B4GALT7* disorders [15].

He underwent a two-staged palatoplasty (13 months and 2 years) which was complicated by wound dehiscence and need for additional surgical revision. Vesicoureteral reflux resolved by 14 months of age. He continued to exhibit axial hypotonia and difficulty bearing weight due to knee instability with frequent patellar joint dislocations and subluxations. He walked at 15 months with the assistance of a walker. He underwent patellar realignment surgery at 6 years and septoplasty at

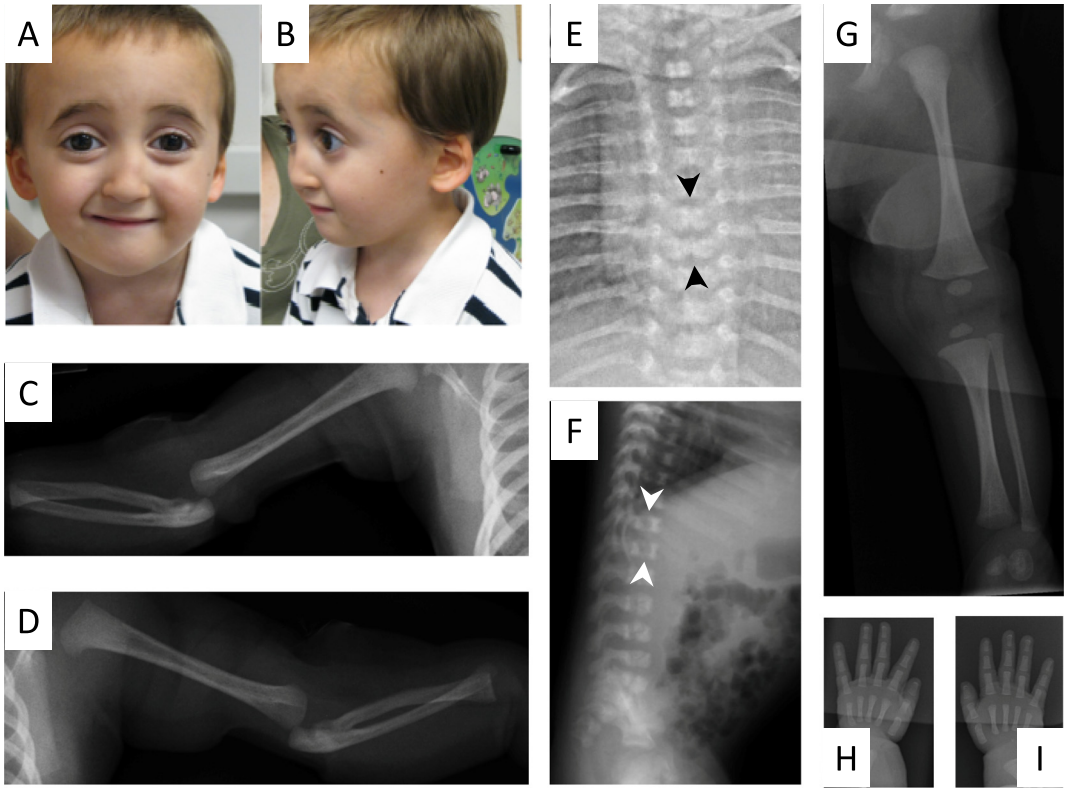

Fig. 1. Photograph of male sibling at age 4 years demonstrates broadened, flat nasal bridge (A) retrognathia, low-set, and posteriorly rotated ears (B). Skeletal survey at 3 weeks of age demonstrates bilateral dislocation of the radial heads, hypoplasia of the distal radii, and bowing of the proximal ulnae (C, D). Anterior/posterior and lateral radiographs of the chest, abdomen, thoracic and lumbar spine (E, F) demonstrate butterfly vertebrae at T7 and T8 (black arrows), and coronal cleft deformities of the vertebral bodies of the thoracic and lumbar spine (white arrows). The intrapedicular distance of the vertebral bodies remains constant from cranial to caudal and do not demonstrate their normal widening. The fibulae are long in length compared to the tibiae (G) with normal femur length. The distal phalanges are elongated on all digits of both hands (H, I).

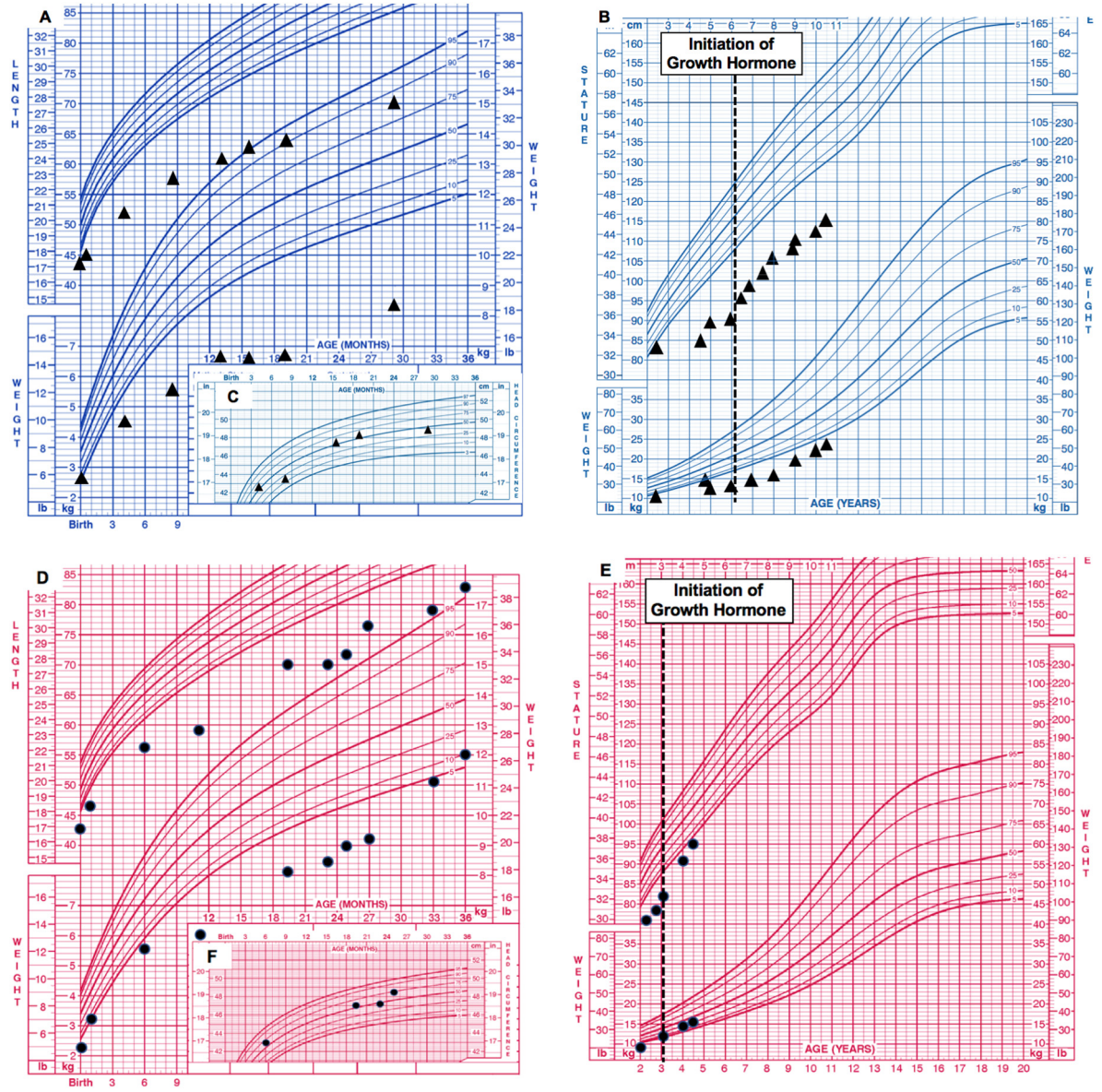

Fig. 2. Center for Disease Control (CDC) growth charts for male sibling (A) birth to 36 months length-for-age and weight-for-age percentiles, and (B) 2–20 years stature-for-age and weight-for age percentiles. Dotted lines indicate initiation of growth hormone (GH) treatment. Head circumference from birth to 36 months demonstrates relative macrocephaly (C). CDC growth charts for female sibling (D) birth to 36 months length-for-age and weight-for-age percentiles, and (E) 2–20 years stature-for-age and weight-for age percentiles. Head circumference from birth to 36 months demonstrates relative macrocephaly (F).

8 years of age for leftward deviation of his inferior nasal septum. He requires bilevel positive airway pressure for treatment of obstructive sleep apnea. Follow-up skeletal survey at 11 years noted resolution of coronal clefts (Fig. S3).

At age 6 years, his weight and height remained below the 1st percentile (weight 12.2 kg, −3.5 S.D. and height 90 cm, −5.2 S.D.) (Fig. 2A, B). Growth hormone provocative testing with clonidine and glucagon demonstrated a peak serum growth hormone of 7.7 μg/L (normal ≥7–10 μg/L) [16–18] and normal cortisol peak (21.9 μg/dL (normal ≥15.8 μg/dL in children with intact HPA axis)) [19]. His insulin like growth factor 1 (IGF-1) level was 2 S.D. below normal (83 ng/mL, normal serum IGF-1 level at Tanner stage 1 is 279 ng/ml ± 92 ng/ml) [20]. Growth hormone treatment (0.3 mg/kg/week) from age 6 years through 11 years was associated with an increase in growth velocity from 5.0 cm/year (1.5 years prior to treatment) to 7.1 cm/year and 8.6 cm/year in the first 2 years of treatment (Fig. 3A) [21]. His bone age (Greulich and Pyle standards) was 6 years at a chronological age of 7 4/12 years. His IGF-1 level was 216 ng/mL (normal) [22]. His height velocity dropped in the subsequent 3 years of growth hormone treatment to 3.0 cm/year, 5.1 cm/year, and 4.9 cm/year during which time his IGF-1 level ranged from 370 to 499 ng/mL. His bone age advanced over the 5 years of growth hormone treatment from 9 years (chronological age of 9 3/12 years) to 12 6/12 years (chronological age of 11 6/12 years) (Fig. 3A). His physical examination at 11 years demonstrated relative macrocephaly: occipitofrontal circumference (OFC) 52.1 cm (40th percentile), height 116 cm (< 1st percentile, −4 S.D.), weight 27 kg (< 1st percentile, −3 S.D.) (Fig. 2B), flattened midface with broad forehead, pointed chin, low-set and overlapping superior helices, bluish sclerae, and micrognathia with abnormally shaped and positioned teeth. His chest was notable for pectus excavatum and right-sided carinatum deformities. Extremities were notable for hypotonia, long and hyper-flexible fingers with positive thumb sign (thumb extends beyond the ulnar border of the hand when overlapped by the fingers) [23], widely spaced first and second toes bilaterally, fifth digit clinodactyly of both feet, and digit 2–3 syndactyly of the right foot. He had no evidence of pubertal initiation (Tanner stage 1) at age 12 8/

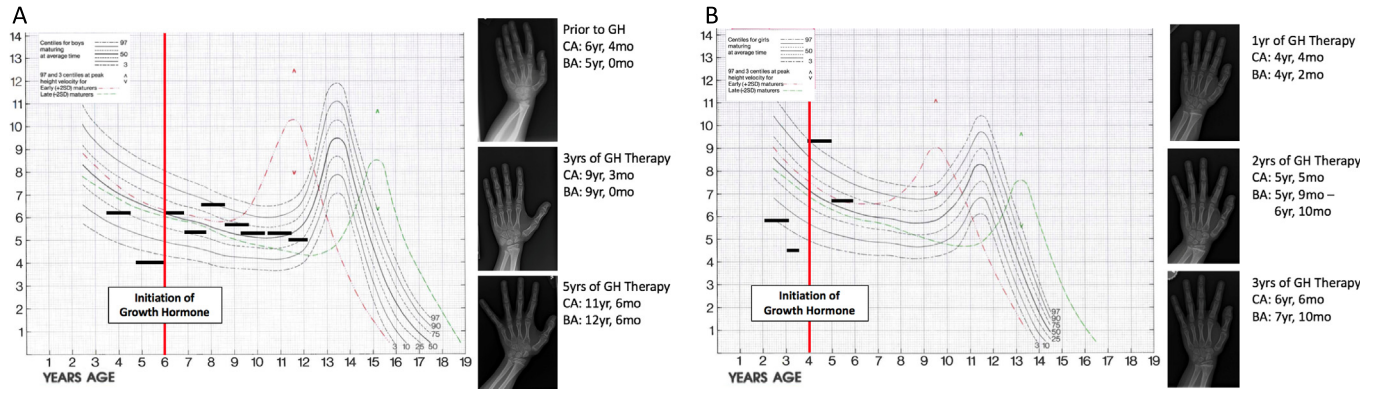

Fig. 3. Growth velocity of male sibling (A) before and after initiation of growth hormone (GH) (red vertical line) with subsequent bone age radiographs demonstrating advancing bone age. Horizontal lines represent time intervals over which growth velocity was calculated. BA - bone age; CA - chronological age; mo - months; yr - years. Growth velocity of female sibling (B) before and after initiation of growth hormone (red vertical line) with subsequent bone ages demonstrating advancing bone age. Horizontal lines represent time intervals over which growth velocity was calculated. Chart adapted from Serono Laboratories, Inc., 100 Longwater Circle, Norwell, MA 02061. (For interpretation of the references to colour in this figure legend, the reader is referred to the web version of this article.)

12 years. His ophthalmological evaluation was unremarkable.

2.1.3. Female sibling

The female sibling was born at 36 weeks' estimated gestation: birth weight 2334 g (27th percentile), length 43.5 cm (12th percentile), and OFC 33 cm (50th percentile) [24]. She shared several facial features with her brother including flattened midface, broad forehead, abnormally folded auriculae, bluish sclerae, retromicrognathia, and widened palpebral fissures. Her palate was intact. Her skeletal survey was notable for radioulnar synostosis, dislocation of the radial heads, mild foreshortening of the proximal left radius, mild dysplasia of the proximal right radius, and coronal clefts of L3, L4 and L5 (Fig. 4). Similar to her brother, the vertebral coronal clefts resolved on subsequent imaging (Fig. S3). CMA and brain MRI were unremarkable; however, skull radiograph at age 4 years demonstrated fusion of the saggital suture (Fig. S4).

At age 2 years, she exhibited poor weight gain (9 kg, < 1st percentile, −3.2 S.D.) and linear growth (71.5 cm, < 1st percentile, −4.1 S.D.) (Fig. 2D, E) which persisted at age 3 7/12 years: weight 11.1 kg (< 1st percentile, −2.9 S.D.), height 78.8 cm (< 1st percentile, −5.0 S.D.), and growth velocity 4.9 cm/year. Growth hormone provocative testing with clonidine and glucagon at age 3 6/12 years demonstrated peak serum growth hormone of 6.0 ng/mL, consistent with growth hormone deficiency based on the guidelines of the Pediatric Endocrine Society and the Growth Hormone Research Society and normal peak cortisol level (25.5 μg/dL) following glucagon stimulation [16–18]. Growth hormone treatment (0.3 mg/kg/week) for 3 years was associated with increases in her height from −4.6 S.D. at age 4 years to −3.7 S.D. and −3.5 S.D. at ages 5 and 6 years, respectively and in her growth velocity (Fig. 3B). Her bone age was 4 2/12 years (chronological age of 4 4/12) and advanced to between 5 9/12 and 6 10/12 years (chronological age 5 5/12 years) (Fig. 3B) during growth hormone treatment.

At age 5 years, she was noted to have relative macrocephaly (OFC 49.9 cm, 35th percentile; weight 15.5 kg, 5th percentile; height 95 cm, < 1st percentile, −3.5 S.D.) [14] (Fig. 2E) with mild frontal bossing, deep-set eyes, mild micrognathia, smooth philtrum, hyperextensible knees with radioulnar synostosis, long fingers with clinodactyly, long toes, and mildly decreased muscle tone. Ophthalmologic examination revealed severe hyperopia corrected with eyeglasses.

Both siblings exhibited motor and speech delays (speaking in single words until age 3 years and full sentences at 5 years). The male sibling

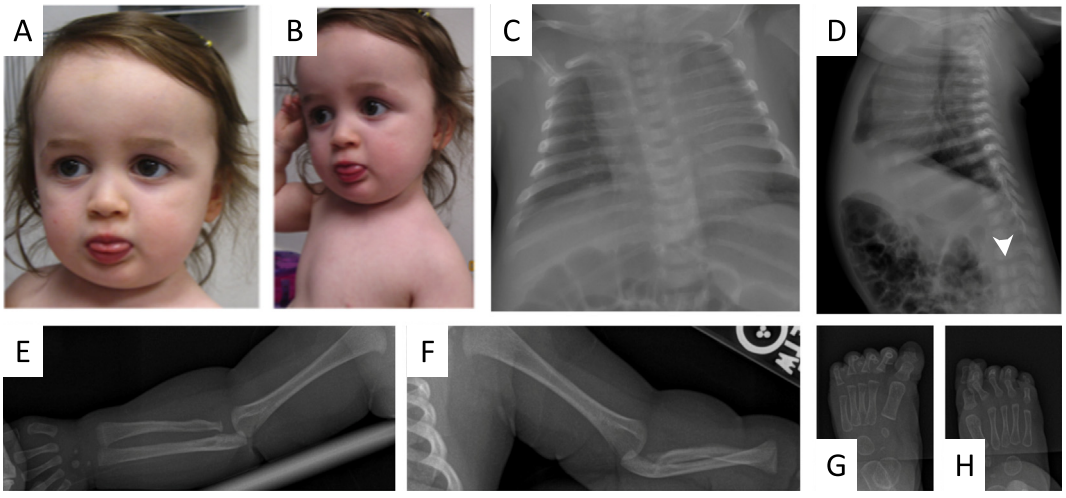

Fig. 4. Photograph of female sibling at age 23 months demonstrates broadened, flat nasal bridge (A) retrognathia, low-set and posteriorly rotated ears (B). Skeletal survey at 1 month of age demonstrates mild levo-curvature of the thoracolumbar spine and coronal clefts in L3, L4, and L5 vertebral bodies (white arrow). Multiple ribs are dysmorphic (C, D). There is mild proximal right radial dysplasia (E). The left arm is notable for negative ulnar variance, mild foreshortening of the proximal radius, proximal radioulnar synostosis, and ulnar dislocation of the radial head; there is mild proximal radial dysplasia and fibrous radioulnar fusion (F). There is bilateral valgus deformity of the great toe interphalangeal joint (G, H).

sat unassisted at 12 months, crawled at 2 years, and walked independently at 3 years. The female sibling walked unassisted at 3.5 years and toilet trained at 5 years. Both siblings required tympanostomy tube placement for frequent ear infections, but neither has hearing loss. The male sibling has difficulties with reading comprehension and thought organization and was diagnosed with attention deficit hyperactivity disorder at age 6 years. He has difficulty with handwriting due to his underlying skeletal abnormalities. Both siblings have received speech/language, occupational, physical, and developmental therapies since infancy.

2.1.4. Bone evaluation

Both siblings report recurrent bone and joint pain without evidence of overt or healing fractures on radiographs. Dual-energy X-ray absorptiometry (DEXA) of the male sibling at age 12 years demonstrated clinically significant osteopenia with reduced bone mineral density of the left total hip (0.586 g/cm^2 (Z-score −2.3), femoral neck (0.487 g/cm^2 (Z-score −3.0), and spine (0.572 g/cm^2, (Z score −1.2). Metabolic bone evaluation at age 11 7/12 years demonstrated increased bone turnover with elevated levels of urine N-terminal telopeptide (NTX) and serum osteocalcin; however, serum and urine calcium homeostasis markers were normal (Table 2) [25–32]. DEXA scan of the female sibling at age 4 9/12 years did not demonstrate significant osteopenia (bone mineral density of total hip 0.477 g/cm^2 (Z score −1.4), femoral neck 0.497 g/cm^2 (Z-score −0.8), and spine 0.512 g/cm^2 (Z-score +0.1)). Metabolic bone evaluation at age 5 5/12 years demonstrated normal serum and urine calcium homeostasis and normal NTX, but increased serum osteocalcin.

3. Results

3.1. Whole exome sequencing (WES) results

Clinical WES of the affected siblings and their parents revealed biallelic, pathogenic variants in *B4GALT7* in both siblings: a maternally inherited missense variant, c.421C > T: p.Arg141Trp, and a paternally inherited missense variant, c.808C > T: p.Arg270Cys. The maternally inherited variant, p.Arg141Trp (NM_00.7255.2; rs187063864), has an allele frequency of 6.5E−05 among European descent individuals in gnomAD (http://gnomad.broadinstitute.org, Accessed March 2019) [33] and is predicted deleterious (CADD score 33). The paternally inherited variant, p.Arg270Cys (rs28937869), is also extremely rare (minor allele frequency 9.7E−05 among European descent individuals) and is predicted deleterious (CADD score 34). Of note, Salter et al. reported a 13 year old unrelated female with the same genotype as these siblings whose phenotype included short stature, hypermobility, radioulnar synostosis, hypotonia, hyperelastic skin, motor delay, pes planus, bowing of limbs, abnormal and delayed healing, without reported cognitive delay, cleft palate, coronal clefts, or osteopenia [1].

Table 2
Results from laboratory evaluation of bone markers in siblings with biallelic, pathogenic B4GALT7 variants.

	Male sibling	Female sibling	Reference range
Serum			
Calcium (mg/dL)	10.1	9.8	M: 9.4–10.3 [25] F: 9.4–10.8 [25]
Calcium, ionized (mg/dL)	5.08	5.03	M: 4.6–5.3 [25] F: 4.9–5.3 [25]
Phosphorus (mg/dL)	5.2	5.1	M: 3.6–5.8 [25] F: 4.5–6.5 [25]
%CK-BB (brain-type creatine kinase) (IU/L)	2	2	5–25 [26]
Alkaline phosphatase (U/L)	289	390	M: 60–450 [25] F: 100–350 [25]
Bone alkaline phoshatase (mcg/L)	95	142	M: 51–164 [27] F: 147–359 [27]
Parathyroid hormone (PTH) (pg/mL)	26	32	9–52 [28]
25-OH vitamin D (ng/mL)	47	41	21–100 [29]
Creatine kinase (U/L)	160	276	M: 55–215 [30] F: 75–230 [30]
Urine (spot)			
Calcium/creatinine ratio	0.12	0.23	M: 0.04–0.7 [25] F: 0.05–1.1 [25]
Phosphorus/creatinine ratio	0.24	0.33	M: 0.8–3.2 [25] F: 1.2–18 [25]
Bone turnover markers			
Serum osteocalcin (ng/mL)	122	136	M: 56–80 [31] F: 66–88 [31]
Urine NTX-telopeptide (nmol/mmol creatinine)	598	628	M: 386–681 [32] F: 646–923 [32]

4. Discussion

Pathogenic variants in *B4GALT7* disrupt proteoglycan synthesis. The clinical features of these siblings (radioulnar synostosis, short stature, delayed motor and cognitive development) are consistent with the phenotypes of previously described individuals [1]. However, the features observed in these siblings (osteopenia, coronal clefts, cognitive delay, cleft palate) that differ from an unrelated affected individual with the same genotype [1] emphasize the phenotypic variability among individuals with biallelic, pathogenic *B4GALT7* variants. Osteopenia has been reported in 5/9 individuals with *B4GALT7*-related disorders who underwent evaluation of bone density, and cleft palate has been reported in 3/32 individuals (Table 1). The vertebral coronal clefts identified in these siblings resolved during childhood. While coronal clefts likely represent variants of delayed normal endochondral ossification [34], they are often identified among infants and children with skeletal dysplasias and chromosomal abnormalities [34,35]. The intrafamilial phenotypic differences between the siblings (cleft palate and hyperopia) as well as interfamilial phenotypic differences between an unrelated affected individual and these siblings (osteopenia, coronal clefts, cognitive delay, cleft palate) may result from genetic background differences (including the chromosome 9p duplication in the male sibling) or hormonal and environmental modifiers.

Originally thought to be a progeroid form of Ehlers-Danlos Syndrome, *B4GALT7*-related disorders are now classified as spondylodysplastic Ehlers Danlos Syndrome (spEDS) [6,36]. Biallelic, pathogenic variants in *B3GALT6* and *SLC39A13* are also grouped with *B4GALT7*-related disorders in the spEDS phenotype due to considerable phenotypic overlap [37] which includes major criteria of short stature, hypotonia, and limb bowing and minor criteria of skin hyperextensibility, pes planus, delayed motor and cognitive development, and osteopenia [6,36]. Phenotypic variability of spEDS may be attributable to allelic and locus heterogeneity [37].

Growth hormone treatment has been infrequently reported among patients with biallelic *B4GALT7* variants and evidence of functional growth hormone deficiency. Guo et al. described a male child with forearm bowing, marked joint flexibility, poor somatic and linear growth, and biallelic *B4GALT7* variants (c.122T > C; p.Leu41Pro and c.808C > T; p.Arg270Cys) who failed to respond to growth hormone treatment after demonstrating a moderate response to growth hormone stimulation and normal thyroid hormone, IGF-1, and IGFBP-3 levels [8]. Growth hormone treatment has not been reported for patients with biallelic *B4GALT7* variants with short stature and normal levels of growth hormone [6,10]. Growth hormone treatment for both siblings was initiated prior to discovery of biallelic, pathogenic *B4GALT7* variants [21]. The long term impact of growth hormone treatment in our patients will require assessment of their adult heights as well as interval changes in bone age. More rapid than expected advancement in bone ages of both siblings during the years after initiation of growth hormone treatment (increase in height Z score) may be mitigated by early

epiphyseal closure. Prediction of adult height from bone age, interpretation of growth hormone stimulation results, and interpretation of effectiveness of growth hormone treatment based on comparisons with standards derived from typical children are confounded by the few other patients with this rare disorder. However, the growth hormone molecule has been shown to have O-glycoslylation with carbohydrate moieties including galactose, so it is possible that the *B4GALT7* variant could affect growth hormone biosynthesis or biological action [38]. Discordance of abnormal bone density assessed by DEXA scan in the male and female siblings suggests possible sex-associated or age-dependent mechanisms of bone density regulation, effect of genetic modifiers, or unidentified environmental differences.

Although our siblings and the majority of reported cases (Table 1) have delayed motor and cognitive development as well as difficulties with learning and behavior, the contributions of pathogenic *B4GALT7* variants to cognition and learning have not been defined. Whether the unusual, maternal knee dislocations represent skeletal or ligamentous abnormalities associated with *B4GALT7* haploinsufficiency is unclear and will require careful phenotypic assessment of a large cohort of heterozygous carriers.

5. Conclusions

Biallelic, pathogenic variants in *B4GALT7* have been associated with spondylodysplastic type of Ehlers-Danlos syndrome. Allelic and locus heterogeneity have been noted among the 30 patients reported in the literature, and the siblings presented here provide additional support to the phenotype variability among patients with B4GALT7-related disorders. We emphasize the radiological phenotype in our patient and note vertebral coronal clefts which have not been previously reported. In addition to the common features of short stature, joint hypermobility, and hypotonia, the male sibling suffers from abnormal wound healing, osteopenia, and cleft palate which are less frequently observed in *B4GALT7* associated spondysplastic Ehlers-Danlos syndrome. The siblings underwent treatment with growth hormone; the long term effects of growth hormone therapy on adult height and bone density among individuals with *B4GALT7* spondylodysplastic are unknown and will require longitudinal studies of these siblings and other affected patients.

Supplementary data to this article can be found online at https://doi.org/10.1016/j.bone.2019.03.029.

Acknowledgements

The authors thank the family and referring physicians for participation in this study. This work was supported by grants from the National Institutes of Health (K08 HL105891 [J.A.W.], K12 HL120002 [F.S.C.]), from the Children's Discovery Institute (FSC), and the Saigh Foundation (FSC).

References

[1] C.G. Salter, J.H. Davies, R.J. Moon, J. Fairhurst, D. Bunyan, D.D.D. Study, N. Foulds, Further defining the phenotypic spectrum of B4GALT7 mutations, Am. J. Med. Genet. A 170 (2016) 1556–1563.
[2] E. Quentin, A. Gladen, L. Roden, H. Kresse, A genetic defect in the biosynthesis of dermatan sulfate proteoglycan: galactosyltransferase I deficiency in fibroblasts from a patient with a progeroid syndrome, Proc. Natl. Acad. Sci. U. S. A. 87 (1990) 1342–1346.
[3] M. Asano, K. Furukawa, M. Kido, S. Matsumoto, Y. Umesaki, N. Kochibe, Y. Iwakura, Growth retardation and early death of beta-1,4-galactosyltransferase knockout mice with augmented proliferation and abnormal differentiation of epithelial cells, EMBO J. 16 (1997) 1850–1857.
[4] C. Rodeheffer, B.D. Shur, Targeted mutations in beta1,4-galactosyltransferase I reveal its multiple cellular functions, Biochim. Biophys. Acta 1573 (2002) 258–270.
[5] Q. Lu, P. Hasty, B.D. Shur, Targeted mutation in beta1,4-galactosyltransferase leads to pituitary insufficiency and neonatal lethality, Dev. Biol. 181 (1997) 257–267.
[6] M. Ritelli, C. Dordoni, V. Cinquina, M. Venturini, P. Calzavara-Pinton, M. Colombi, Expanding the clinical and mutational spectrum of B4GALT7-spondylodysplastic Ehlers-Danlos syndrome, Orphanet J. Rare Dis. 12 (2017) 153.
[7] T. Arunrut, M. Sabbadini, M. Jain, K. Machol, F. Scaglia, A. Slavotinek, Corneal clouding, cataract, and colobomas with a novel missense mutation in B4GALT7-a review of eye anomalies in the linkeropathy syndromes, Am. J. Med. Genet. A 170 (2016) 2711–2718.
[8] M.H. Guo, J. Stoler, J. Lui, O. Nilsson, D.W. Bianchi, J.N. Hirschhorn, A. Dauber, Redefining the progeroid form of Ehlers-Danlos syndrome: report of the fourth patient with B4GALT7 deficiency and review of the literature, Am. J. Med. Genet. A 161A (2013) 2519–2527.
[9] M. Faiyaz-Ul-Haque, S.H. Zaidi, M. Al-Ali, M.S. Al-Mureikhi, S. Kennedy, G. Al-Thani, L.C. Tsui, A.S. Teebi, A novel missense mutation in the galactosyltransferase-I (B4GALT7) gene in a family exhibiting facioskeletal anomalies and Ehlers-Danlos syndrome resembling the progeroid type, Am. J. Med. Genet. A 128A (2004) 39–45.
[10] H. Kresse, S. Rosthoj, E. Quentin, J. Hollmann, J. Glossl, S. Okada, T. Tonnesen, Glycosaminoglycan-free small proteoglycan core protein is secreted by fibroblasts from a patient with a syndrome resembling progeroid, Am. J. Hum. Genet. 41 (1987) 436–453.
[11] F. Cartault, P. Munier, M.L. Jacquemont, J. Vellayoudom, B. Doray, C. Payet, H. Randrianaivo, J.M. Laville, A. Munnich, V. Cormier-Daire, Expanding the clinical spectrum of B4GALT7 deficiency: homozygous p.R270C mutation with founder effect causes Larsen of Reunion Island syndrome, Eur. J. Hum. Genet. 23 (2015) 49–53.
[12] W.J. Kent, C.W. Sugnet, T.S. Furey, K.M. Roskin, T.H. Pringle, A.M. Zahler, D. Haussler, The human genome browser at UCSC, Genome Res. 12 (2002) 996–1006.
[13] M. Kircher, D.M. Witten, P. Jain, B.J. O'Roak, G.M. Cooper, J. Shendure, A general framework for estimating the relative pathogenicity of human genetic variants, Nat. Genet. 46 (2014) 310–315.
[14] C.D. Fryar, Q. Gu, C.L. Ogden, K.M. Flegal, Anthropometric reference data for children and adults: United States, 2011–2014, Vital Health Stat. 3 (2016) 1–46.
[15] V.A. McKusick, Mendelian inheritance in man and its online version, OMIM, Am. J. Hum. Genet. 80 (2007) 588–604.
[16] Society, G.R, Consensus guidelines for the diagnosis and treatment of growth hormone (GH) deficiency in childhood and adolescence: summary statement of the GH Research Society, J. Clin. Endocrinol. Metab. 85 (2000) 3990–3993.
[17] . Grimberg, A., DiVall, S.A., Polychronakos, C., Allen, D.B., Cohen, L.E., Quintos, J. B., Rossi, W.C., Feudtner, C., Murad, M.H., Drug, et al. (2016). Guidelines for growth hormone and insulin-like growth factor-I treatment in children and adolescents: growth hormone deficiency, idiopathic short stature, and primary insulin-like growth factor-I deficiency. Horm. Res. Paediatr. 86, 361–397.
[18] J. Nakamoto, Chapter 12: Pediatric laboratory testing for specific endocrine conditions, in: A. Moyer, R. Brown (Eds.), Pediatric Laboratory Medicine, McGraw-Hill Education, Inc, 2017.
[19] N. Weintrob, A.S. Davidov, A.S. Becker, G. Israeli, A. Oren, O. Eyal, Serum free cortisol during glucagon stimulation test in healthy short-statured children and adolescents, Endocr. Pract. 24 (2018) 288–293.
[20] Hasegawa, Y., Hasegawa, T., Aso, T., Kotoh, S., Tsuchiya, Y., Nose, O., Ohyama, Y., Araki, K., Tanaka, T., Saisyo, S., et al. (1993). Comparison between insulin-like growth factor-I (IGF-I) and IGF binding protein-3 (IGFBP-3) measurement in the diagnosis of growth hormone deficiency. Endocr. J. 40, 185–190.
[21] J.M. Tanner, P.S. Davies, Clinical longitudinal standards for height and height velocity for North American children, J. Pediatr. 107 (1985) 317–329.
[22] Greulich, W. Radiographic Atlas of Skeletal Development of the Hand and Wrist. (Stanford University Press).
[23] F. De Maio, A. Fichera, V. De Luna, F. Mancini, R. Caterini, Orthopaedic aspects of Marfan syndrome: the experience of a referral center for diagnosis of rare diseases, Adv Orthop 2016 (2016) 8275391.
[24] T.R. Fenton, A new growth chart for preterm babies: Babson and Benda's chart updated with recent data and a new format, BMC Pediatr. 3 (2003) 13.
[25] Pediatric Nephrology, Springer, Berlin, Heidelberg, 2009.
[26] Cabaniss, C.D. (1990). Creatine kinase. In Clinical Methods: The History, Physical, and Laboratory Examinations, rd, H.K. Walker, W.D. Hall, and J.W. Hurst, eds. (Boston).
[27] J. Jurimae, Interpretation and application of bone turnover markers in children and adolescents, Curr. Opin. Pediatr. 22 (2010) 494–500.
[28] S. Turan, B. Topcu, I. Gokce, T. Guran, Z. Atay, A. Omar, T. Akcay, A. Bereket, Serum alkaline phosphatase levels in healthy children and evaluation of alkaline phosphatase z-scores in different types of rickets, J. Clin. Res. Pediatr. Endocrinol. 3 (2011) 7–11.
[29] J.Y. Lee, T.Y. So, J. Thackray, A review on vitamin d deficiency treatment in pediatric patients, J. Pediatr. Pharmacol. Ther. 18 (2013) 277–291.
[30] D.B. Andropoulos, Pediatric normal laboratory values, in: D.B.A. George, A. Gregory (Eds.), Gregory's Pediatric Anesthesia, Fifth edition, Blackwell Publishing Ltd., 2012.
[31] M. Cioffi, A.M. Molinari, P. Gazzerro, B. Di Finizio, M. Fratta, A. Deufemia, G.A. Puca, Serum osteocalcin in 1634 healthy children, Clin. Chem. 43 (1997) 543–545.
[32] A.M. Bollen, D.R. Eyre, Bone resorption rates in children monitored by the urinary assay of collagen type I cross-linked peptides, Bone 15 (1994) 31–34.
[33] Lek, M., Karczewski, K.J., Minikel, E.V., Samocha, K.E., Banks, E., Fennell, T., O'Donnell-Luria, A.H., Ware, J.S., Hill, A.J., Cummings, B.B., et al. (2016). Analysis of protein-coding genetic variation in 60,706 humans. Nature 536, 285–291.
[34] J. Westvik, R.S. Lachman, Coronal and sagittal clefts in skeletal dysplasias, Pediatr. Radiol. 28 (1998) 764–770.
[35] E. Doberentz, R. Schumacher, U. Gembruch, J.A. Gasser, A.M. Muller, Coronal vertebral clefts: a radiological indicator for chromosomal aberrations, Pediatr. Dev. Pathol. 16 (2013) 1–6.

[36] Malfait, F., Francomano, C., Byers, P., Belmont, J., Berglund, B., Black, J., Bloom, L., Bowen, J.M., Brady, A.F., Burrows, N.P., et al. (2017). The 2017 international classification of the Ehlers-Danlos syndromes. Am. J. Med. Genet. C Semin. Med. Genet. 175, 8–26.

[37] Brady, A.F., Demirdas, S., Fournel-Gigleux, S., Ghali, N., Giunta, C., Kapferer-Seebacher, I., Kosho, T., Mendoza-Londono, R., Pope, M.F., Rohrbach, M., et al. (2017). The Ehlers-Danlos syndromes, rare types. Am. J. Med. Genet. C Semin. Med. Genet. 175, 70–115.

[38] J.J. Bustamante, L. Gonzalez, C.A. Carroll, S.T. Weintraub, R.M. Aguilar, J. Munoz, A.O. Martinez, L.S. Haro, O-glycosylated 24 kDa human growth hormone has a mucin-like biantennary disialylated tetrasaccharide attached at Thr-60, Proteomics 9 (2009) 3474–3488.